URSI GASS 2021, Rome, Italy, 28 August - 4 September 2021

Exploiting Topological Properties of Mie-Resonance-Based Hybrid Metasurfaces for Ultrafast Switching of Light Polarization

Yuhao Wu(1), Lei Kang(1), Sawyer D. Campbell(1)
Pingjuan L. Werner (1), Douglas H. Werner* (1)
(1) Department of Electrical Engineering and Center for Nanoscale Science
The Pennsylvania State University, University Park, PA, 16802, USA

Abstract

Mie resonances of high-index dielectric matesurfaces provide large freedom for light modulation with low loss, which, by including a highly reflective backplane, induce an enhanced optical magnetism with increasing quality factor. In this paper, we show that Mie-resonance-based α-Si:H metasurfaces with a gold backplane can be utilized to manipulate light polarization upon reflection. The nontrivial topological properties associated with the scattering field are revealed by reflection matrix analysis. Topologically protected polarization conversion is demonstrated by varying the incident wavevector. Furthermore, the nonlinear modeling shows that such hybrid metasurfaces can realize ultrafast all-optical polarization switching of near-infrared light. The topological nature of the metasurface's response offers great flexibility in polarization generation and dynamic modulation.

1 Introduction

Light polarization variation that spawns from light-matter interaction has been widely used in the fields of optical metrology, communications, material characterizations, etc. However, the corresponding devices based on traditional methods are intrinsically difficult to miniaturize and actively switch. Therefore, the development of devices with ultrafast dynamic control of polarization at the chip-scale is highly desired. Metasurfaces, the 2D counterparts to metamaterials, have demonstrated their ability to achieve sophisticated control over all intrinsic features of optical waves [1]–[5]. More importantly, metasurfaces consisting of subwavelength resonators can be designed to minimize the thermo-optical effect, which makes them suitable for ultrafast switching [6]–[11]. On the other hand, there has been increasing interest in exploring the topological nature of the Bloch-mode inside periodic photonics structures inspired by a topological analysis of the solid-state system. The non-radiative Bloch-modes, with an extreme quality (Q) factor, exhibit themselves as the vortex singularities at the high-symmetry point in momentum space, have been intensively studied [12]–[17]. Here, we study the topological nature of the light reflected by a Mie-resonance-based α-Si:H hybrid metasurface. We demonstrate its potential for ultrafast optical polarization switching by exploiting carrier dynamics in the α-Si resonators.

2 Optical Response of an Ideal System

First, the physical mechanism of the hybrid metasurface was analyzed by studying the band diagram of an ideal lossless system. As the inset of Fig. 1(a) shows, the unit cell consists of a nanodisk (ε_{ND} = 12, diameter (D) = 0.9a, height (h) = 0.4a) on top of a perfect electric conductor (PEC). The band diagram is calculated in COMSOL by its internal eigenmode solver. The color-coded dispersion curve indicates the radiation loss (ratio between the radiation power and the guided power) of the corresponding mode. The mode profiles of the Re(E_z) on the first band at $k_{\|}$ = (0.06,0.06)2π/a and $k_{\|}$ = (0.06,0)2π/a are depicted in Fig. 1(b)(c). Odd parity of the mode can be identified accordingly with $k_{\|}$ along the ΓM direction, while even parity modes can be identified along the ΓX direction. The mode parity is governed by the C_{4v} symmetry of the lattice, which is of great importance in explaining the light-matter interaction and the polarization conversion during the scattering process. The odd and even resonance modes couple to s-pol and p-pol radiation states, respectively. According to the temporal coupled mode theory [18], [19], there is an intermediate mode between these modes that achieves a complete polarization conversion, when the coupling coefficients associated with s-pol and p-pol reflections are equal, referred to as the critical coupling condition.

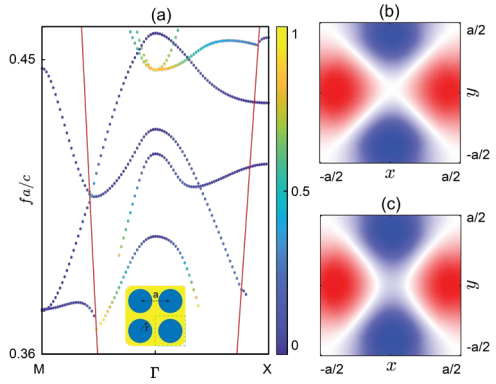

Figure 1. A hybrid metasurface for all-optical ultrafast switching of light polarization. (a) Band diagram of an ideal metasurface. The unit cell consists of a lossless nanodisk (ε_{ND} = 12) on top of a PEC backplane. The color-coded markers show the radiation loss of the system, while the red lines denote the light cone. (b)(c) Eigenmode profile

for Re(E_z) at $k_{||}$ = (0.06, 0.06)2π/a and $k_{||}$ = (0.06, 0)2π/a for the first non-radiative band.

Fig. 2 shows the simulated reflection behavior of the lossless system under *s*-pol plane wave illumination with wavevector $k = (k_{||}, k_z)$, where $k_{||} = (k_x, k_y)$, as illustrated in the inset of Fig. 2(a). The reflectance spectra of the *p*- and *s*-polarized components at $k_{||,1}$ = (0.06,0.026)2π/a, which corresponds to the critical coupling condition for the first band, are shown in Fig. 2(a), indicating complete polarization conversion at an eigenfrequency ω_1 = 0.3947(2πc/a). A high Q factor of 119 is derived from the spectra. Here, the reflectance at ω_1 is also mapped as a function of $k_{||}$. In Fig. 2(b), the reflection coefficient vector field, *i.e.*, (Re(r_{ss}), Im(r_{ss})) indicated by the grey vectors, is plotted above the color-coded reflectance, R_{ss}. Clearly, four singularity points of zero reflectance can be identified in the vector field with a saddle point of winding number -1, and a source point of +1. Meanwhile, $k_{||,1}$ = (0.06,0.026)2π/a and its mirror component are located at a pair of singularity points with opposite winding numbers, which is consistent with the symmetry property of the metasurface. These singularity points, referred to as topological charges, reveal the topological nature of the scattering process. The rapid variation of polarization properties around these charges provides great potential for the generating and tailoring of light polarization. Furthermore, the polarization rotation angle γ, which denotes the rotation of the major axis of the polarization ellipse relative to the *s*-polarized incident light, and the corresponding ellipticity χ of the polarization ellipse are presented in Fig. 2(c),(d). A sign flipping phenomenon of γ and χ is observed with respect to the $k_x = k_y$ plane. This is attributed to the reflection coefficient relation $r_{sp}(k_x, k_y)$ = - $r_{sp}(k_y, k_x)$ and $r_{ss}(k_x, k_y)$ = $r_{ss}(k_y, k_x)$, which arises from the reciprocity and C_{4v} rotational symmetry of the metasurface. Apparently, an abundance of polarization states can be realized around the topological charges, which will be demonstrated in the following sections by studying the ultrafast modulation of α-Si:H resonator-based systems using nonlinear dynamics.

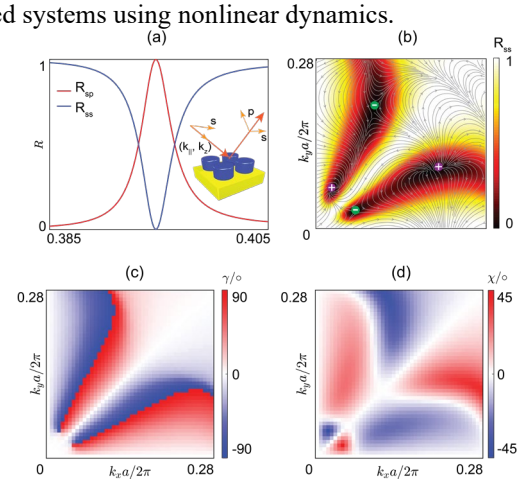

Figure 2. (a) Reflectance spectrum of the lossless metasurface illuminated by *s*-polarized light at $k_{||,1}$ = (0.06,0.026)2π/a. (b) R_{ss} and the corresponding reflection coefficient vector flow (Re(r_{ss}), Im(r_{ss})) versus incident wavevectors for *s*-polarized incident light at ω_1. (c),(d) The corresponding polarization rotation angle (γ) and the ellipticity (χ) at ω_1.

3 Hybrid Metasurfaces Based on α-Si:H Nanodisks Patterned on Gold

The resonance mechanism and the topological nature of the scattered field are explored in the previous section within the context of an ideal lossless system. However, the practicality of this study will be tested by the introduction of inevitable losses of metals in the near-infrared region. Therefore, the metasurface formed by an array of α-Si:H nanodisks (a = 620 nm, $D = 2h = 0.8a$) and an optically thick gold substrate is studied at the first band with the same methodology used in the previous section. α-Si:H resonators have been previously demonstrated to support strong Mie resonances. Meanwhile, these structures have been shown to facilitate all-optical ultrafast modulations due to their large nonlinearity and fast carrier dynamics [9]. It has been shown that optical excitations at photon energies higher than the band-gap of *a*-Si:H may induce changes in both the real and imaginary parts of the material's refractive index [9]. Recently, a theoretical model has been developed to described the dynamic processes in *a*-Si:H metasurfaces by comprehensively including all primary nonlinear processes (*i.e.*, two-photon absorption (TPA), free-carrier injection and relaxation, and lattice heating) under pulsed laser excitation [20]. This theoretical approach accurately reproduces all nonlinear features captured by experiments, showing that the maximum modulation is primarily determined by the peak (real and imaginary) permittivity change in *a*-Si:H, while the modulation dynamics are controlled by the competition between the three nonlinear processes. Therefore, we first study the static response of the hybrid metasurface as well as the response due to the maximum permittivity change within the perturbative region ($\Delta\varepsilon \ll \varepsilon$). This is not only instructive for temporal nonlinear processes, but also reveals the variation of the topological property under perturbation.

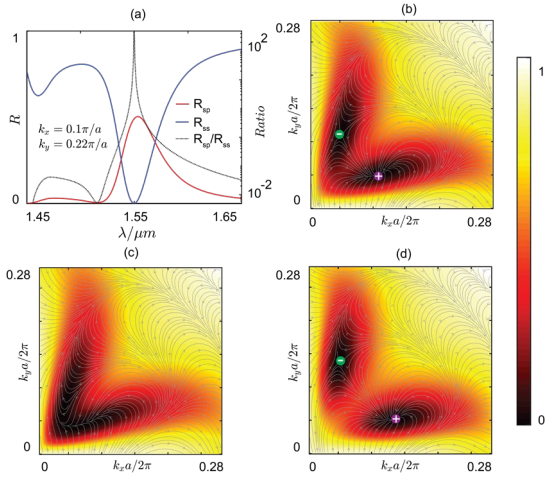

Figure 3. (a) Reflectance spectrum for an *s*-polarized incident wave at $k_{||}$ = (0.05,0.11)2π/a. The black dashed

curve denotes the ratio between R_{sp} and R_{ss}. (b),(c),(d) R_{ss} and the corresponding reflection coefficient vector flow at 1550 nm, when $\varepsilon_{ND} = \varepsilon_{Si}$, $\varepsilon_{ND} = \varepsilon_{Si} - 0.1$ and $\varepsilon_{ND} = \varepsilon_{Si} + 0.1$, respectively.

Figure 3(a) provides the reflection spectrum of the α-Si:H hybrid metasurface at $k_{||}$ = (0.05,0.11)2π/a, the critical coupling point. A zero of R_{ss} can be identified at 1550 nm where a more than 300-times contrast is observed, indicating a high efficiency polarization modulation around 1550 nm. R_{sp} reaches a peak value of ~0.5 at a slightly longer wavelength. Compared with the ideal system, both the spectral degradation and the frequency shift of the R_{sp} peak comes from the material loss, which is consistent with the temporal coupling mode theory analysis. In Fig. 3(b), the reflection coefficient vector flow at 1550 nm reveals the topological properties by two topological charges of -1 and +1, which, like in the lossless system, is symmetric with respect to the plane $k_x = k_y$. Active polarization manipulation of the metasurface is investigated by introducing a permittivity variation ($\Delta\varepsilon$) of -0.1 and 0.1 (within the perturbative region) in the *a*-Si:H nanodisks, as shown in Fig. 3(c),(d). Compared with the unperturbed system, the increase in permittivity drives the opposite singularities to move away from each other, *i.e.* ($k_{||}$ = (0.05,0.11)2π/a) to (0.052,0.138)2π/a). On the other hand, the decrease will lead to a drift of the singularities towards each other and an annihilation, which implies that complete polarization conversion disappears. This non-trivial variation of the topological property suggests that even moderate permittivity changes can significantly influence how the polarization states spawn around these singularities.

4 Ultrafast Switching of Light Polarization

In this section, we investigate the ultrafast nonlinear responses of the proposed metasurface by utilizing the nonlinear model presented by in Ref [20]. A 100fs laser pulse at 800 nm with pump fluence of F = 100 μJ/cm^2 (10% of that used in [9], [20]) is assumed to excite the α-Si:H/gold hybrid metasurface, which induces a permittivity change of -0.02+0.02*i*. The probe light is an *s*-polarized plane wave whose in-plane wave vector is $k_{||}$. Here, we sequentially present the ultrafast intensity modulation and the dynamic polarization state switching effect.

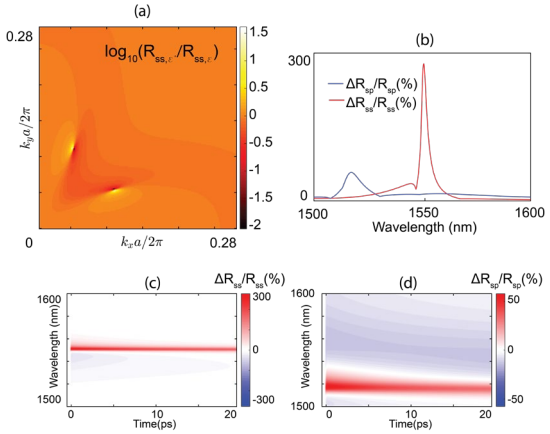

Figure 4. (a) Static reflectance ratio defined as $\log_{10}(R_{ss,\varepsilon'_{ND}}/R_{ss,\varepsilon_{ND}})$ associated with two scenarios, *i.e.*, $\varepsilon_{ND} = \varepsilon_{Si}$ and $\varepsilon'_{ND} = \varepsilon_{Si} + \Delta\varepsilon$, where $\Delta\varepsilon = -0.02 + 0.02i$. (b) The corresponding spectra of the static reflectance ratio for both *s*- and *p*-polarized components at $k_{||}$ = (0.05,0.11)2π/a. (c),(d) Transient reflectance modulation as a function of probe wavelength and time delay between the pump and probe pulses.

Figure 4(a) illustrates the ratio between the static R_{ss} when $\varepsilon_{ND} = \varepsilon_{Si}$ (unperturbed) and $\varepsilon'_{ND} = \varepsilon_{Si} + \Delta\varepsilon$. The logarithm mapping highlights two areas associated with the R_{ss} zeros in the unperturbed state (bright spots) and the perturbed state (dark spots). In addition, Fig. 4(b) further illustrates the static differential reflectance ($\Delta R_{ss}/R_{ss}$ and $\Delta R_{sp}/R_{sp}$) at $k_{||}$ = (0.05,0.11)2π/a as a function of wavelength, indicating a maximum modulation of more than 200 times for R_{ss} around 1550 nm. Furthermore, a maximum transient differential reflectance $\Delta R_{ss}/R_{ss}$ ($\Delta R_{sp}/R_{sp}$) larger than 200 % (50 %) is identified around the resonance at 1550 nm (1520 nm) in Fig. 4(c),(d). They all feature a decay time of ~20 ps, which originates from the competition between the fast free carrier relaxation and the slow phonon scattering effect.

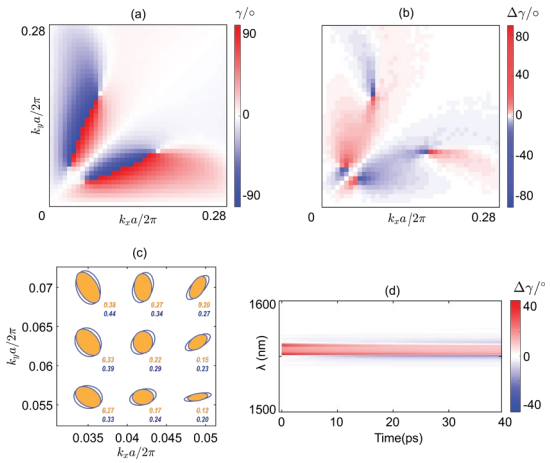

Figure 5. (a) Polarization rotation angle γ as a function of incident wavevectors at 1550 nm when $\varepsilon_{ND} = \varepsilon_{Si}$. (b) The differential polarization rotation angle $\Delta\gamma$ when $\Delta\varepsilon = -0.02 + 0.02i$.(c) The corresponding polarization ellipses of the reflected waves around $k_{||}$ = (0.042,0.063)2π/*a* when ε_{ND} =

ε_{Si} (yellow) and $\varepsilon'_{ND} = \varepsilon_{Si} + \Delta\varepsilon$ (open). The red (blue) outline color of the ellipses indicates the right (left) handedness of the elliptical polarization. (d) Transient rotation angle modulation as a function of probe wavelength and time delay between the pump and probe pulses.

In Fig. 2, we have observed the capability of the lossless metasurface to synthesize diverse polarization behavior upon reflection. In Fig. 5(a), the polarization rotation angle γ of the unperturbed system is also in $k_{\|}$ space with the same symmetry property. More importantly, γ exhibits pronounced modulation when the *a*-Si:H was pumped with the same fluence of 100 fs at 800 nm as shown in Fig. 5(b). With the rapid polarization variation around the topological charge, we identified a $k_{\|} = (0.042,0.063)2\pi/a$, where the rotation angle experienced the strongest modulation. A maximum rotation angle modulation ($\Delta\gamma$) of 40° was identified at this $k_{\|}$, as depicted in Fig. 5(c). The dynamics of γ switching across the spectrum was also studied at this wavevector. At wavelengths around the resonance at 1550 nm, $\Delta\gamma$ experiences a peak value of ~ 40° and a long decay time. Surprisingly, at 1560.3 nm, the maximum $\Delta\gamma$ reaches ~30° along with a short decay time constant of ~40 ps. These results strongly indicate the potential of the proposed α-Si:H hybrid metasurface to serve as a platform for strong and diverse polarization manipulations.

5 Acknowledgements

This work was supported in part by the Penn State MRSEC, Center for Nanoscale Science, under Award No. NSF DMR-1420620 and by the Defense Advanced Research Projects Agency (DARPA) (HR00111720032).

6 References

1. H.-T. Chen, A. J. Taylor, and N. Yu, "A Review of Metasurfaces: Physics and Applications," *Rep. Prog. Phys.*, **79**, 7, p. 076401, Jun. 2016, doi: 10.1088/0034-4885/79/7/076401.

2. S. Chang, X. Guo, and X. Ni, "Optical Metasurfaces: Progress and Applications," *Annu. Rev. Mater. Res.*, **48**, 1, pp. 279–302, Jul. 2018, doi: 10.1146/annurev-matsci-070616-124220.

3. D. Lin, P. Fan, E. Hasman, and M. L. Brongersma, "Dielectric Gradient Metasurface Optical Elements," *Science*, **345**, 6194, pp. 298–302, Jul. 2014, doi: 10.1126/science.1253213.

4. A. Arbabi, Y. Horie, M. Bagheri, and A. Faraon, "Dielectric Metasurfaces for Complete Control of Phase and Polarization with Subwavelength Spatial Resolution and High Transmission," *Nature Nanotechnology*, **10**, 11, pp. 937–943, Nov. 2015, doi: 10.1038/nnano.2015.186.

5. J. P. Balthasar Mueller, N. A. Rubin, R. C. Devlin, B. Groever, and F. Capasso, "Metasurface Polarization Optics: Independent Phase Control of Arbitrary Orthogonal States of Polarization," *Phys. Rev. Lett.*, **118**, 11, p. 113901, Mar. 2017, doi: 10.1103/PhysRevLett.118.113901.

6. L. H. Nicholls *et al.*, "Ultrafast Synthesis and Switching of Light Polarization in Nonlinear Anisotropic Metamaterials," *Nature Photon*, **11**, 10, pp. 628–633, Oct. 2017, doi: 10.1038/s41566-017-0002-6.

7. Y. Yang *et al.*, "Femtosecond optical polarization switching using a cadmium oxide-based perfect absorber," *Nature Photon*, **11**, 6, pp. 390–395, Jun. 2017, doi: 10.1038/nphoton.2017.64.

8. M. Taghinejad *et al.*, "Ultrafast Control of Phase and Polarization of Light Expedited by Hot-Electron Transfer," *Nano Lett.*, **18**, 9, pp. 5544–5551, Sep. 2018, doi: 10.1021/acs.nanolett.8b01946.

9. M. R. Shcherbakov *et al.*, "Ultrafast All-Optical Switching with Magnetic Resonances in Nonlinear Dielectric Nanostructures," *Nano Lett.*, **15**, 10, pp. 6985–6990, Oct. 2015, doi: 10.1021/acs.nanolett.5b02989.

10. Y. Yang, I. I. Kravchenko, D. P. Briggs, and J. Valentine, "All-dielectric metasurface analogue of electromagnetically induced transparency," Nature Communications, 5, 1, p. 5753, Dec. 2014, doi: 10.1038/ncomms6753.

11. L. Kang, H. Bao, and D. H. Werner, "Interference-Enhanced Optical Magnetism in Surface High-Index Resonators: A Pathway toward High-Performance Ultracompact Linear and Nonlinear Meta-optics," *Photon. Res.*, **7**, 11, p. 1296, Nov. 2019, doi: 10.1364/PRJ.7.001296.

12. B. Zhen, C. W. Hsu, L. Lu, A. D. Stone, and M. Soljačić, "Topological Nature of Optical Bound States in the Continuum," *Phys. Rev. Lett.*, **113**, 25, p. 257401, Dec. 2014, doi: 10.1103/PhysRevLett.113.257401.

13. E. N. Bulgakov and D. N. Maksimov, "Optical Response Induced by Bound States in the Continuum in Arrays of Dielectric Spheres," *J. Opt. Soc. Am. B*, **35**, 10, p. 2443, Oct. 2018, doi: 10.1364/JOSAB.35.002443.

14. K. Koshelev, S. Lepeshov, M. Liu, A. Bogdanov, and Y. Kivshar, "Asymmetric Metasurfaces with High- Q Resonances Governed by Bound States in the Continuum," *Phys. Rev. Lett.*, **121**, 19, p. 193903, Nov. 2018, doi: 10.1103/PhysRevLett.121.193903.

15. E. N. Bulgakov and D. N. Maksimov, "Bound States in the continuum and Polarization Singularities in Periodic Arrays of Dielectric Rods," *Phys. Rev. A*, **96**, 6, p. 063833, Dec. 2017, doi: 10.1103/PhysRevA.96.063833.

16. Z. Sadrieva, K. Frizyuk, M. Petrov, Y. Kivshar, and A. Bogdanov, "Multipolar Origin of Bound States in the Continuum," *Phys. Rev. B*, **100**, 11, p. 115303, Sep. 2019, doi: 10.1103/PhysRevB.100.115303.

17. W. Chen, Y. Chen, and W. Liu, "Singularities and Poincaré Indices of Electromagnetic Multipoles," *Phys. Rev. Lett.*, **122**, 15, p. 153907, Apr. 2019, doi: 10.1103/PhysRevLett.122.153907.

18. Y. Guo, M. Xiao, and S. Fan, "Topologically Protected Complete Polarization Conversion," *Phys. Rev. Lett.*, **119**, 16, p. 167401, Oct. 2017, doi: 10.1103/PhysRevLett.119.167401.

19. S. Fan, W. Suh, and J. D. Joannopoulos, "Temporal Coupled-Mode Theory for the Fano Resonance in Optical Resonators," *J. Opt. Soc. Am. A*, **20**, 3, p. 569, Mar. 2003, doi: 10.1364/JOSAA.20.000569.

20. G. Della Valle *et al.*, "Nonlinear Anisotropic Dielectric Metasurfaces for Ultrafast Nanophotonics," *ACS Photonics*, **4**, 9, pp. 2129–2136, Sep. 2017, doi: 10.1021/acsphotonics.7b00544.